

# A Compact Ultra Wideband Antenna with Triple-Sense Circular Polarization

Guihong Li, Huiqing Zhai, Tong Li, Long Li, Changhong Liang  
School of Electronic Engineering, Xidian University  
Xi'an, 710071, China, guihonger@sina.com

**Abstract**—In this letter, a new compact antenna design with triple-sense circular polarization (CP) is presented for ultra-wideband (UWB) communication applications. The UWB property is obtained by utilizing a compact complementary planar monopole. In order to achieve multiband CP waves on base of UWB operation, the measurement has been taken such as etching a T-shaped slit in the antenna ground and adding a rectangular parasitic stub to the antenna radiator. The antenna has been fabricated and measured. Good agreement is achieved between the simulation and measurement, which shows that the presented antenna covers the UWB operation from 3.1GHz to 11.8GHz with good CP waves at Worldwide Interoperability for Microwave Access (WiMAX) (3.63-3.77 GHz bands) for left hand CP (LHCP), the wireless local area network band (WLAN) (4.95-5.18 GHz bands) for right hand CP (RHCP), and X band (9.55-9.97 GHz bands) for left hand CP (LHCP).

## I. INTRODUCTION

In recent decades, circularly polarized (CP) antennas have received much attention for finding applications in satellite positioning, radio frequency identification (RFID) and sensor systems with the development of modern wireless communication. To be resistant to the depolarization effects, bad weather conditions and multi path propagation, it is imperative for the antennas to have CP characteristics, which is insensitive to the respective orientations on the useful frequency operation when applied to launch and receive electromagnetic waves. CP waves can be generated when two degenerate modes of equal amplitude and phase difference of  $90^\circ$  are excited. Right-hand circular polarization (RHCP) and left-hand circular polarization (LHCP) can be defined by a  $90^\circ$  phase lead and lag, respectively. In [1]-[6], various techniques were proposed for multiband CP patch antenna designs. For example, eight rectangular perturbations with unequal length in [1] or two asymmetric pentagonal slots in [2] were introduced to excite a pair of degenerate modes for CP radiation. By loading a pair of L-shaped stubs outside the truncated patch, an outer mode and an inner mode were excited respectively [3]. In [4], the dual-band circular polarization was provided by dual resonant elements. In [5], a novel broadband monopole antenna with dual band CP radiation was presented using a ground plane embedded with an inverted-L slit. Furthermore, a triple band CP antenna was proposed in [6] by utilizing two ring slots and an L-shaped feed line.

Since the Federal Communications Commission (FCC) specifies the unlicensed 3.1-10.6 GHz band for ultra-wideband (UWB) commercial usages in 2002 [7], the increasing

demands have stimulated many researches into UWB technology because of its low cost, low power consumption, high data transmission rates, resistance to severe multipath and jamming, etc. Meanwhile, antenna designs for UWB applications are facing many challenges including the miniaturized design, impedance matching, radiation stability, and electromagnetic interference (EMI) problems [8]-[10]. As is known, the printed monopoles are widely utilized to design the UWB antennas due to their attractive features such as simple structure, low profile, light weight, wide impedance bandwidth, and omnidirectional radiation patterns. However, the radiation patterns of the printed monopole antennas are always linearly polarized while is difficult to radiate CP radiation. Thus, a monopole antenna design which can generate both the LP and CP waves is an interesting issue that is worthy of being researched.

In this letter, a new monopole antenna design with triple-sense CP radiation property is proposed for UWB application. The research is based on a circular-shaped monopole antenna which covers UWB operation. By employing a T-shaped slit in the ground and a rectangular parasitic stub on the edge of the radiator, triple-sense CP radiation at the centre frequency of 3.7, 5.1, and 9.7 GHz are generated, which belong to Worldwide Interoperability for Microwave Access (WiMAX), wireless local area network (WLAN), and X bands. The employment of T-shaped slit and the rectangular parasitic stub to the basic circular-shaped monopole can obtain the triple-sense CP radiation while keeping the UWB property. Since a 50-Ohm feed line connected to an impedance transformer is adopted, the matching of the proposed antenna is improved. Meanwhile, the introduced T-shaped slit and the rectangular parasitic stub hasn't occupied the more space, leading to a miniaturized design. Furthermore, the antenna's performances are investigated according to the key parameters, from which we can find the antenna's controllable characteristics.

## II. ANTENNA DESIGN

Fig.1 (a) shows the geometry of the presented UWB antenna with CP radiation in WiMAX/WLAN/X wireless communication design. The photograph of the fabricated antenna is displayed in Fig.1 (b). The antenna is fabricated on a dielectric substrate with relative permittivity of 4.4 and loss tangent of 0.024. The antenna is designed with the overall size of  $27\text{mm} \times 27\text{mm} \times 1\text{mm}$ , where the size of the ground plane is  $27\text{mm} \times 9\text{mm}$  and the radius of the circular radiation patch is 8.5mm. The detailed design dimensions are listed in Tab. 1. In

this letter, a 50-Ohm feed line of width 2mm and length 3mm is terminated with SMA connector to improve the impedance matching of the antenna. Compared with traditional UWB antenna, the presented antenna obtains triple-sense CP waves by embedding a T-shaped slit in the ground plane, and adding a rectangular parasitic stub in the circular radiation patch. Through the antenna's performance analysis, the introduction of the T-shaped slit and rectangular parasitic stub can redistribute the magnetic currents in the slot so that two orthogonal resonant modes with equal amplitude and a 90° phase difference can be excited for CP operation.

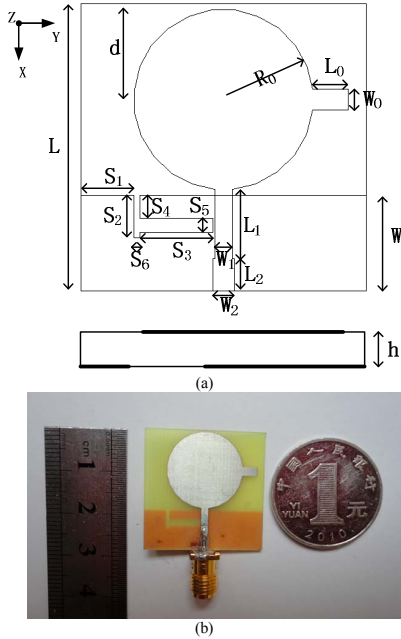


Figure 1. (a) Configuration of the presented antenna (b) Fabricated prototype.

To investigate the operation of resonant modes, surface current distributions on the antenna at 3.7, 5.1, and 9.7 GHz are presented in Fig. 2. In Fig. 2(a), maximum currents are localized mainly in the ground to produce resonant modes at 3.7 GHz. At 5.1 GHz, the ground and patch both contribute to the resonance from Fig. 2(b). In Fig. 2(c), the maximum current is distributed mainly along the rectangular parasitic stub in the circular patch to excite the resonant mode at 9.7 GHz. Fig. 2 shows that the three resonant modes of the antenna are influenced by the ground embedded with T-shaped slit and the patch connected with a parasitic stub. In other words, the T-shaped slit and the rectangular parasitic stub can be used to excite triple CP radiation.

TABLE I  
DIMENSIONS OF THE OPTIMIZED ANTENNA DESIGN

| Parameters     | (mm) | Parameters     | (mm) |
|----------------|------|----------------|------|
| L              | 27   | S <sub>1</sub> | 5    |
| L <sub>0</sub> | 3.46 | S <sub>2</sub> | 4    |
| L <sub>1</sub> | 6.5  | S <sub>3</sub> | 6.9  |
| L <sub>2</sub> | 3    | S <sub>4</sub> | 2.2  |
| W              | 9    | S <sub>5</sub> | 1.3  |
| W <sub>0</sub> | 2    | S <sub>6</sub> | 0.6  |
| W <sub>1</sub> | 1.6  | R <sub>0</sub> | 8.5  |
| W <sub>2</sub> | 2    | d              | 9    |

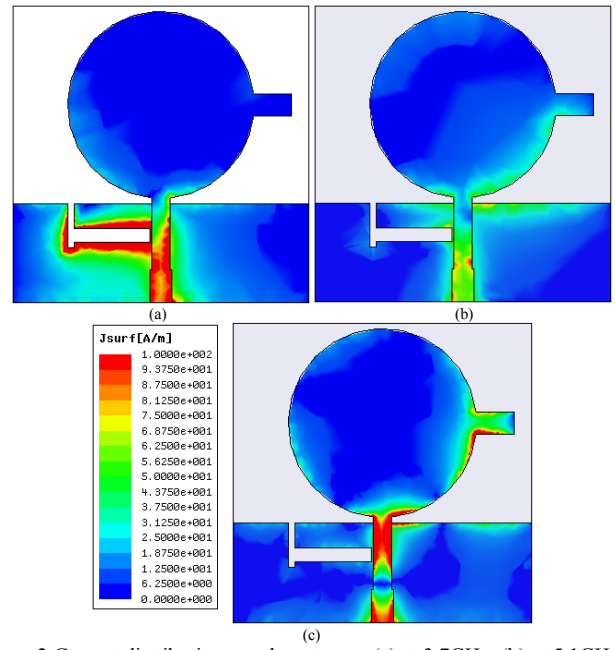


Figure 2 Current distributions on the antenna. (a) at 3.7GHz, (b) at 5.1GHz, (c) at 9.7GHz.

The two CP characteristics at lower frequencies are determined by the size of the T-shaped slit, while the CP wave at upper frequency is controlled by the size of the rectangular stub, which will be discussed in the following section. In this design, the upper CP frequency is approximated by

$$f_0 = c/4L_0\sqrt{\epsilon_r} \quad (1)$$

where  $c$  is velocity of light,  $L_0$  is the length of the rectangular stub, and  $\epsilon_r$  is the relative dielectric constant of the substrate. Given a desired CP resonance frequency, one can use Eq. (1) to define the initial total size of the stub for an initial design. Here, the stub in the radiator is designed with the side width of 2mm and length of 3.46mm. The measurement is carried out by using Agilent E8357A vector network analyzer. The measured simulated S11 results of the proposed UWB antennas with triple-band CP radiation are shown in Fig.3, which have good agreement with simulated result carried out by the full-wave electromagnetic software Ansoft High Frequency Structure Simulator (HFSS) [11]. According to the measured results, it can be found that the proposed compact antenna can effectively cover the impedance bandwidths of 3.1-11.8GHz, which can well satisfy the UWB band.

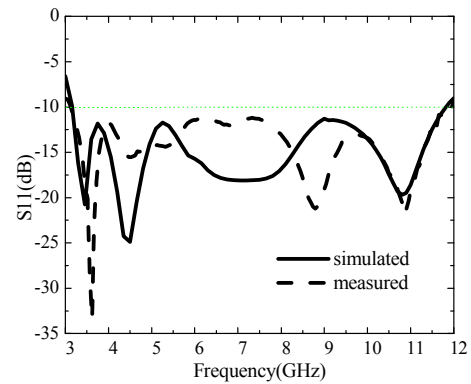


Figure 3 Measured and simulated return losses.

Fig. 4 depicts illustrates the measured and simulated AR against frequency in the +Z direction at the desired CP operation bands. It can be seen that the presented antenna can achieve CP radiations at WiMAX band from 3.63 to 3.77 GHz, WLAN band from 4.95 to 5.18 GHz, and X band from 9.55 to 9.97 GHz. The 3-dB AR bandwidths at WiMAX band, WLAN band, and X-band are 3.78%, 4.54%, and 4.3%, respectively. The reflection coefficients in these bands are all below -10 dB. The measured result is in good agreement with numerical prediction. The variation of the measured and simulated results is possibly caused by the rough welded joint of the SMA connector, the leakage current of the coaxial cable, and anechoic chamber measurement error.

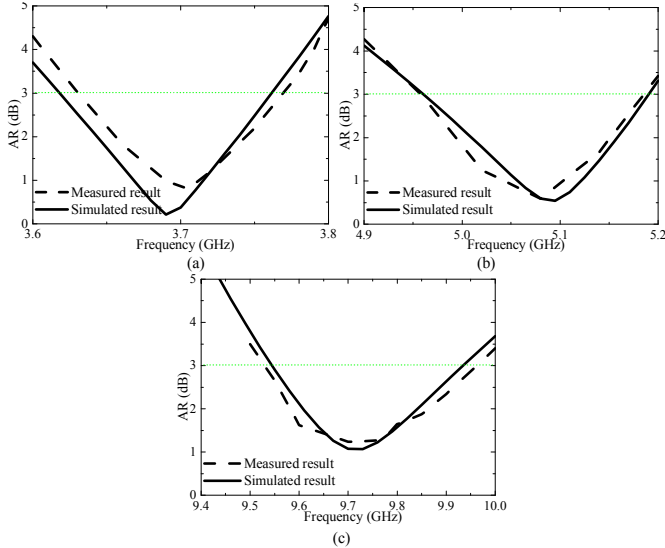


Figure 4 Measured and simulated AR at CP operating bands. (a) WIMAX band, (b) WLAN band, (c) X band.

Fig. 5-7 display the measured normalized radiation patterns at 3.7, 5.1, and 9.7 GHz in the x-z and y-z planes, respectively. The measured radiation patterns of the antenna include RHCP and LHCP components. The figures show that reasonably good LHCP radiations at 3.7 and 9.7 GHz along with good RHCP radiation at 5.1 GHz are realized according to the comparison of RHCP and LHCP components. It is noted that the radiation patterns are not omnidirectional because the proposed antennas is not symmetrical and the radiation patterns are influenced by the employed slit and stub. The measured peak gain is 1.8 dBic at 3.7 GHz, 2.5 dBic at 5.1 GHz, and 3.8 dBic at 9.7 GHz.

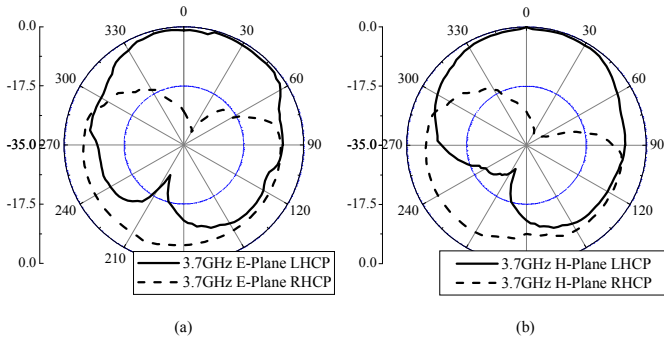


Figure 5 Measured radiation pattern at 3.7 GHz. (a) on XZ-plane, (b) on YZ-plane.

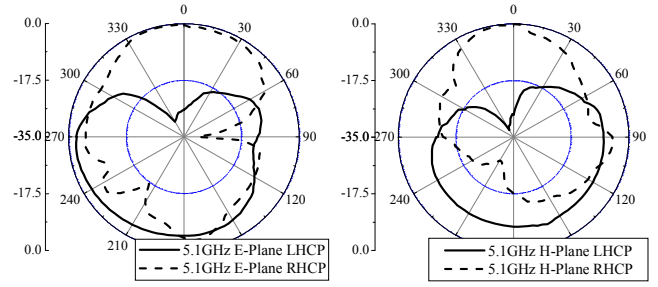


Figure 6 Measured radiation pattern at 5.1 GHz. (a) on XZ-plane, (b) on YZ-plane.

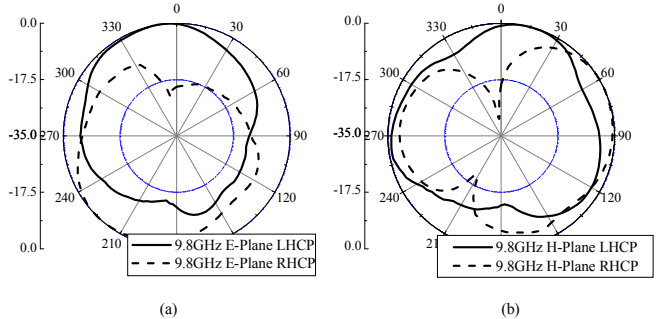


Figure 7 Measured normalized radiation patterns at 9.7 GHz. (a) on XZ-plane, (b) on YZ-plane.

### III. PARAMETRIC ANALYSIS

For further investigation, the vital parameters of the antenna are discussed to find their impacts on the AR characteristics in the triple CP bands. The lengths of L-shaped slit arms  $S_2$ ,  $S_3$  and the parasitic stub length  $L_0$  are especially examined to study their influences on the AR property. All the parameters keep their initial values unless stated. To note, the S11 curve is always less than -10 dB in the UWB band, which is insensitive to the parameter variation.

Fig. 8 shows the effects of various dimensions of  $S_2$  on the triple CP bands. In Fig. 8, it is observed that the AR frequency center of CP operations shifts downwards in WiMAX band, whereas AR results are affected slightly in WLAN/X band when  $S_2$  increases. Fig. 9 shows the effects of various  $S_3$  on the triple CP bands. It can be seen that the AR frequency center of CP operations tends to decrease at WiMAX/WLAN band, but moves little in X band with the increase of  $S_3$ . The influence of  $L_0$  on AR results is shown in Fig. 9. The value of  $L_0$  is decreased from 3.66 to 3.26 mm progressively. It is observed that the AR results get worse in X band and have nearly no change in WiMAX/WLAN bands.

From Fig. 8-10, it can be seen that the desired CP bands are mainly controlled by the added T-shaped slit and parasitic stub. Specifically, the WiMAX band is mainly controlled by the parameter  $S_2$  and  $S_3$ , WLAN band is mainly controlled by  $S_3$  and  $L_0$ , and X band depend mainly on  $L_0$ . The above result can verify the current analysis in the upper section. Therefore, we can easily change their dimensions for the desired CP bands without the need to redesign the whole antenna.

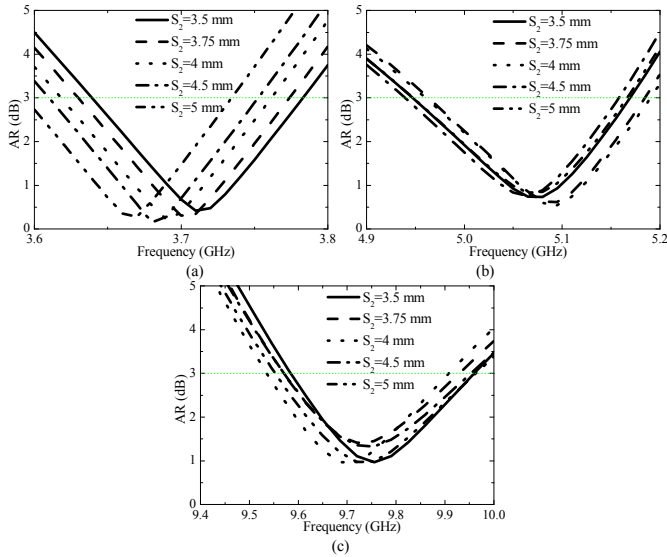


Figure 8 Simulated AR of various  $S_2$ .

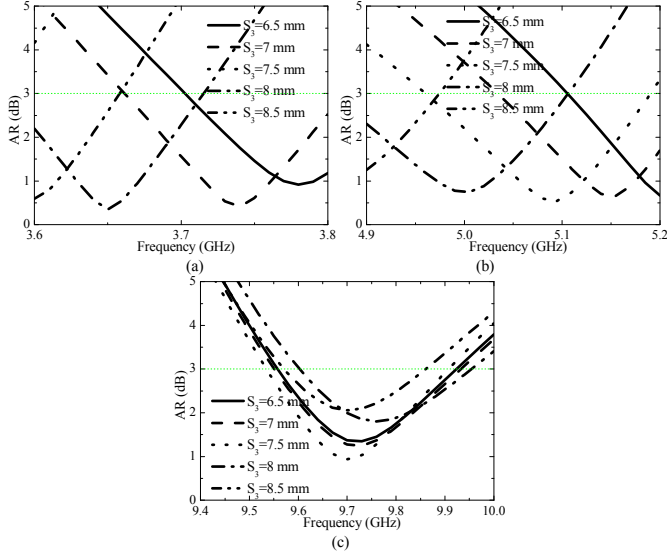


Figure 9 Simulated AR of various  $S_3$ .

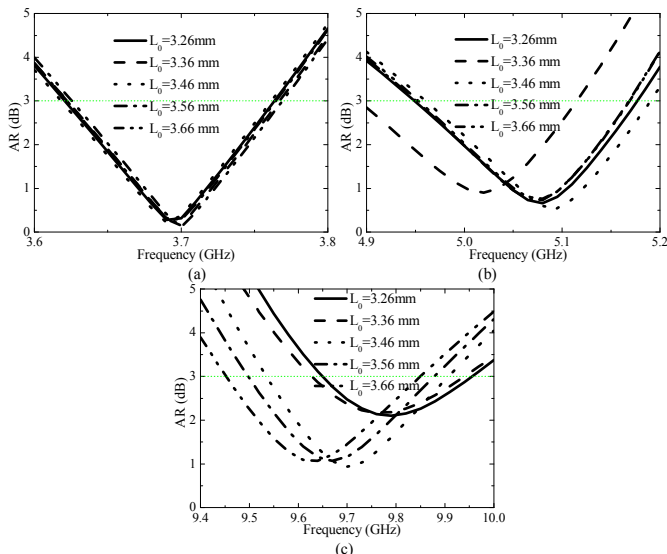


Figure 10 Simulated AR of various  $L_0$ .

#### IV. CONCLUSION

A triple-sense circularly polarized UWB antenna is presented in this research, which is obtained by embedding a T-shaped slot element in the ground plane and adding a rectangular stub element in the monopole structure. The measured and simulated values for the antenna designs verify their predicted performance characteristics, including small size, easy fabrication, UWB impedance bandwidth, triple-sense CP characteristics. Parametric analysis shows that the above characteristics can be modified by adjusting antenna sizes to provide CP radiation in other useful bands.

#### ACKNOWLEDGMENT

This work is supported by the NSFC under Contract No.61101066 and the Fundamental Research Funds for the Central Universities, and partially supported by the Program for New Century Excellent Talents in University of China, the NSFC under Contract No.61072017, Natural Science Basic Research Plan in Shaanxi Province of China (No.2010JQ8013), and Foundation for the Returned Overseas Chinese Scholars, State Education Ministry and Shaanxi Province.

#### REFERENCES

- [1] S. A. Rezaeieh, "Dual band dual sense circularly polarized monopole antenna for GPS and WLAN applications," *Electron. Lett.*, vol. 47, pp. 1212-1214, October 2011.
- [2] Y. Sung, "Dual-Band Circularly Polarized Pentagonal Slot Antenna," *IEEE Antennas Wireless Propag. Lett.*, vol. 10, pp. 259-261, April 2011.
- [3] C. H. Chen and E. K. N. Yung, "A Novel Unidirectional Dual-Band Circularly-Polarized Patch Antenna," *IEEE Trans. Antennas Propag.*, vol. 59, pp. 3052-3057, August 2011.
- [4] C. Deng, Y. Li, Z. Zhang, G. Pan, and Z. Feng, "Dual-Band Circularly Polarized Rotated Patch Antenna With a Parasitic Circular Patch Loading," *IEEE Antennas Wireless Propag. Lett.*, vol. 12, pp. 492-495, April 2013.
- [5] C. F. Jou, J. W. Wu and C. J. Wang, "Novel broadband monopole antennas with dual-band circular polarization," *IEEE Trans. Antennas Propag.*, vol. 57, pp. 1027-1034, April 2009.
- [6] L. Wang, Y. X. Guo, and W. Sheng, "Tri-Band Circularly Polarized Annular Slot Antenna for GPS and CNSS Applications," *IEEE Early Access Articles*.
- [7] First Report and Order FCC, Federal communications commission revision of part 15 of the commission's rules regarding ultra-wideband transmission systems, FCC, 2002.
- [8] G. Teni, N. Zhang, J. Qiu, and P. Zhang, "Research on a Novel Miniaturized Antipodal Vivaldi Antenna With Improved Radiation," *IEEE Antennas Wireless Propag. Lett.*, vol. 12, pp. 417-420, April 2013.
- [9] E. A. Akbari, M. N. Azarmanesh, and S. Soltani, "Design of miniaturised band-notch ultra-wideband monopole-slot antenna by modified half-mode substrate-integrated waveguide," *IET Microw. Antennas Propag.*, vol. 7, pp. 26-34, March 2013.
- [10] F. Fereidoony, S. Chamaani, and S. A. Mirtaheri, "Systematic Design of UWB Monopole Antennas With Stable Omnidirectional Radiation Pattern," *IEEE Antennas Wireless Propag. Lett.*, vol. 11, pp. 752-755, July 2012.
- [11] High Frequency Structure Simulator (HFSS). Ansoft Corp., Pittsburgh, PA.